



## L-Dopa synthesis using tyrosinase immobilized on magnetic beads

Sevinc Tuncagil<sup>a</sup>, Senem Kiralp Kayahan<sup>a</sup>, Gulay Bayramoglu<sup>b</sup>, M. Yakup Arica<sup>c</sup>, Levent Toppare<sup>a,\*</sup>

<sup>a</sup> Department of Chemistry, Middle East Technical University, 06531 Ankara, Turkey

<sup>b</sup> Department of Chemistry, Gazi University, 06500 Teknik Okullar, Ankara, Turkey

<sup>c</sup> Department of Biology, Gazi University, 06500 Teknik Okullar, Ankara, Turkey

### ARTICLE INFO

#### Article history:

Received 5 September 2008

Received in revised form 18 December 2008

Accepted 18 December 2008

Available online 27 December 2008

#### Keywords:

Magnetic beads

Enzyme immobilization

Tyrosinase

L-Dopa synthesis

### ABSTRACT

Magnetic beads were prepared via suspension polymerization of glycidyl methacrylate (GMA) and methyl methacrylate (MMA) in the presence of ferric ions. Following polymerization, thermal co-precipitation of the Fe(III) ions in the beads with Fe(II) ions under alkaline condition resulted in encapsulation of Fe<sub>3</sub>O<sub>4</sub> nano-crystals within the polymer matrix. The magnetic beads were activated with glutaraldehyde, and tyrosinase enzyme was covalently immobilized on the support via reaction of amino groups under mild conditions. The immobilized enzyme was used for the synthesis of L-Dopa (1-3,4-dihydroxy phenylalanine) which is a precursor of dopamine. The immobilized enzyme was characterized by temperature, pH, operational and storage stability experiments. Kinetic parameters, maximum velocity of the enzyme ( $V_{max}$ ) and Michaelis–Menten constant ( $K_m$ ) values were determined as 1.05 U/mg protein and 1.0 mM for 50–75  $\mu$ m and 2.00 U/mg protein and 4.0 mM for 75–150  $\mu$ m beads fractions, respectively. Efficiency factor and catalytic efficiency were found to be 1.39 and 0.91 for 75–150  $\mu$ m beads and 0.73 and 0.75 for 50–75  $\mu$ m beads fractions, respectively. The catalytic efficiency of the soluble tyrosinase was 0.37. The amounts of immobilized protein were on the 50–75  $\mu$ m and 75–150  $\mu$ m fractions were 2.7 and 2.8 mg protein/g magnetic beads, respectively.

© 2008 Elsevier B.V. All rights reserved.

### 1. Introduction

Naturally occurring amino acid 1-3,4-dihydroxyphenylalanine (L-Dopa) is a precursor of dopamine and an important neural message transmitter [1]. It has been a preferred drug for the treatment of Parkinson's disease since 1967 [2,3]. Decrease in concentration of dopamine in the substantia nigra of the brain causes Parkinson disease [4,5]. Dopamine cannot be used as a drug for Parkinson disease since it is unable to cross the blood–brain barrier whereas L-Dopa can [6]. Therefore, the analysis of tyrosinase activity is important for detecting melanoma cells and Parkinson disease.

Tyrosinase (EC 1.14.18.1; mushroom tyrosinase) is a multifunctional copper-containing enzyme widely distributed in nature. Mushroom tyrosinase is a tetrameric enzyme, and its molecular size is 128 kDa. Enzyme has two distinct substrate binding sites; one with a high affinity for aromatic compounds including phenolic substrates, the other for metal-binding agents and oxygen [7]. Tyrosinase catalyzes two reactions through separate active sites: (1) it catalyses the orthohydroxylation of monophenols, commonly

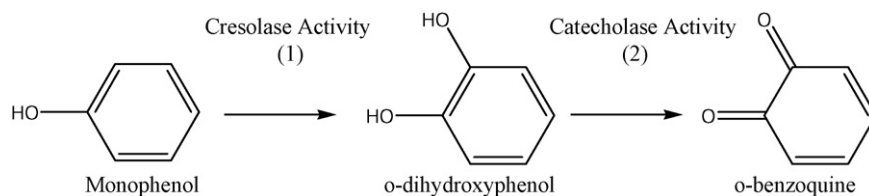
referred as the cresolase activity and (2) it catalyses the oxidoreduction of orthodiphenols to orthoquinones commonly referred as the catecholase activity [8–10] (Scheme 1). The first enzymatic reaction of tyrosinase on tyrosine is proposed by Raper [11]. He proposed oxygen consuming reaction pathway beginning with L-tyrosine, which is oxidized via L-Dopa to dopaquinone.

In recent years it is found that tyrosinase is the rate-limiting enzyme for melanogenesis [12]. It catalyses the hydroxylation of L-tyrosine to L-Dopa via cresolase activity and oxidoreduction of L-Dopa to dopaquinone via catecholase activity. To prevent conversion of L-Dopa to dopaquinone, L-ascorbic acid is added to the reaction medium. In the presence of ascorbic acid the dopaquinone is reduced to L-Dopa while ascorbic acid is oxidized to dehydroascorbic acid [13]. Several matrices [14–17] were used for the immobilization of enzymes. Tyrosinase was immobilized on different matrices [18–25] and they were used for synthesis of L-Dopa (Scheme 2).

There are reports claiming that random covalent immobilization may not promote any additional conformational stability on immobilized enzyme activity, whereas multipoint covalent immobilization might become more stable compared to soluble counterpart or random immobilization. In multipoint covalent immobilization, the active three-dimensional structure of the enzyme could be preserved on the support via multipoint attachment. Thus, the enzyme could be more stable against harsh reaction

\* Corresponding author at: Department of Chemistry, Middle East Technical University, Ortadoğu Teknik Üniversitesi, Kimya Bolumu, 06531 Ankara, Turkey. Tel.: +90 312 2103251; fax: +90 312 2103200.

E-mail address: [toppare@metu.edu.tr](mailto:toppare@metu.edu.tr) (L. Toppare).



**Scheme 1.** Representation of reactions of polyphenol oxidase.

conditions such as heat, organic solvents or any other distorting agents [26–34]. The immobilization of enzymes inside porous supports may increase the enzyme stability by preventing any intermolecular process (proteolysis, aggregation) and by preventing the enzyme from interactions with external interfaces (air, oxygen, immiscible organic solvents, etc.) [27,28]. It should be noted that glutaraldehyde activated supports can stabilize the three-dimensional active conformational network of the immobilized enzyme via multipoint covalent attachment under very mild experimental conditions. In this immobilization method, the amino groups of the enzyme can react with the aldehyde groups which were introduced via modification of the support [35–37].

Magnetic supports have recently been used for immobilization of enzymes [38–44]. Magnetic beads, small globular, iron oxide containing particles, are available at diameter sizes of nanometers up to hundreds of micrometers. Paramagnetic materials like  $\text{Fe}_2\text{O}_3$  are used to prevent aggregation. An iron oxide magnetite core provides the paramagnetic attraction of the particles. The covalent immobilization of an enzyme to magnetic beads can be effective to advance the enzyme stability. Magnetic beads have wide range of applications in the immobilization of cells and enzymes [45], bio-separation systems [46], immunoassays [47], and biosensors [48]. Besides the merits of other supports, magnetic ones can be more easily recovered from the reaction medium, cultivation media and waste from food or fermentation industries [46]. In addition, rotational and vibrational movements are observed in the alternating magnetic fields by polymeric beads exhibiting magnetically anisotropic properties. In a continuous fluidized bed reactor, these magnetic phenomena could be used for preventing product film formation around the enzyme-magnetic beads by an alternating magnetic field. In such a system, vibrating the reaction medium around the support could facilitate substrate transfer through the surface of the enzyme-beads and this fact could also provide a key for controlling immobilized enzyme activity in bioreactor. In addition, the magnetic support could be easily separated from the reaction medium and stabilized in a fluidized bed reactor by applying a magnetic field. The use of magnetic beads could also reduce capital and operation costs [35,36].

In this work, magnetic beads poly(GMA–MMA) were synthesized using monomers glycidyl methacrylate (GMA) and

methyl methacrylate (MMA) (cross-linked with ethyleneglycol dimethacrylate(EGDMA)). Epoxy groups of the magnetic poly(GMA–MMA) beads were converted into amino groups in the presence of ammonia during thermal precipitation of iron oxide crystals. The aminated magnetic beads were used for the immobilization of tyrosinase after activation with glutaraldehyde. The immobilization of tyrosinase on two different size fraction of the magnetic poly(GMA–MMA) beads was investigated. The resultant immobilized tyrosinase was characterized and used for the batch-wise synthesis of L-Dopa from L-tyrosine.

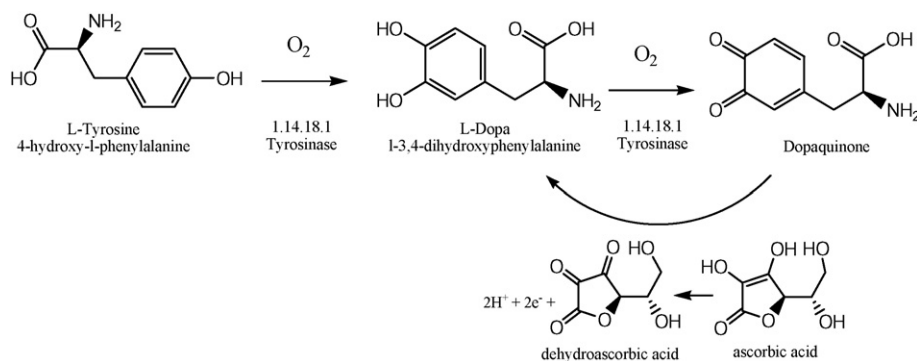
## 2. Experimental

### 2.1. Reagents

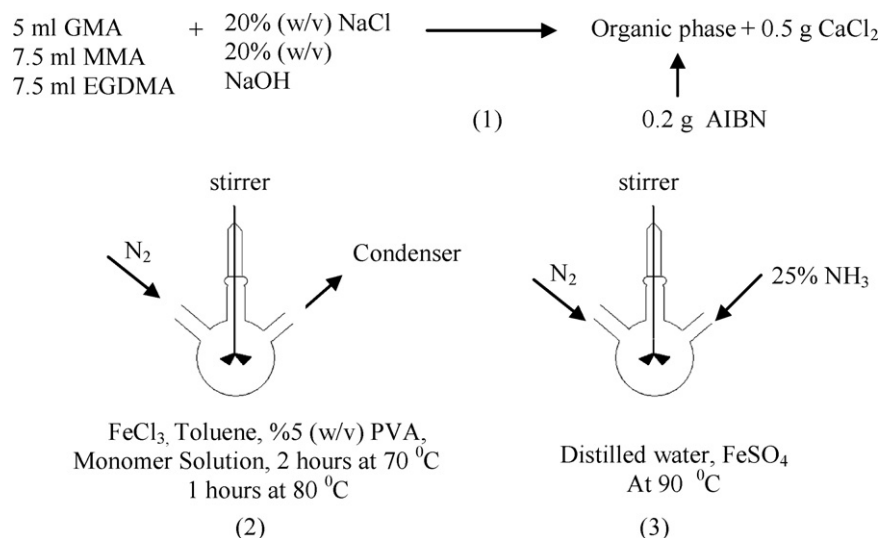
Tyrosinase (o-diphenol;  $\text{O}_2$  oxidoreductase; EC 1.14.18.1 obtained from mushroom as lyophilized powder), L-tyrosine, L-ascorbic acid, hydrochloric acid, sodium hydroxide, sodium molybdate, and sodium nitrite were purchased from Sigma–Aldrich Chem. Co. Glycidyl methacrylate, methyl methacrylate, ethyleneglycol dimethacrylate and  $\alpha$ - $\alpha'$ -azo-isobisbutyronitrile (AIBN) were obtained from Fluka AG. Glutaraldehyde was purchased from Merck. The monomers GMA and MMA distilled under reduced pressure in the presence of hydroquinone and stored at 4 °C.

### 2.2. Preparation of magnetic beads

Magnetic beads were prepared from GMA and MMA via suspension polymerization in the presence of a cross-linker (i.e., ethylene dimethylmethacrylate) as reported previously [41]. Organic phase in 20 mL toluene consists of GMA (7.5 mL), MMA (7.5 mL), EGDMA (7.5 mL; as a cross-linker) and 5.0% polyvinyl alcohol (20 mL, as the stabilizer) and  $\alpha$ - $\alpha'$ -azo-isobisbutyronitrile (0.2 g) were mixed. The continuous phase was prepared in aqueous medium containing the precursor of  $\text{FeCl}_3$  for the thermal iron oxide precipitation in the beads. Polymerization reactor was placed in a water bath and heated to 65 °C. The polymerization reaction was continued at 70 °C for 2.0 h and then at 80 °C for 1.0 h. The resultant beads were filtered under suction and washed with distilled water and ethanol.



**Scheme 2.** Representation of L-Dopa synthesis.



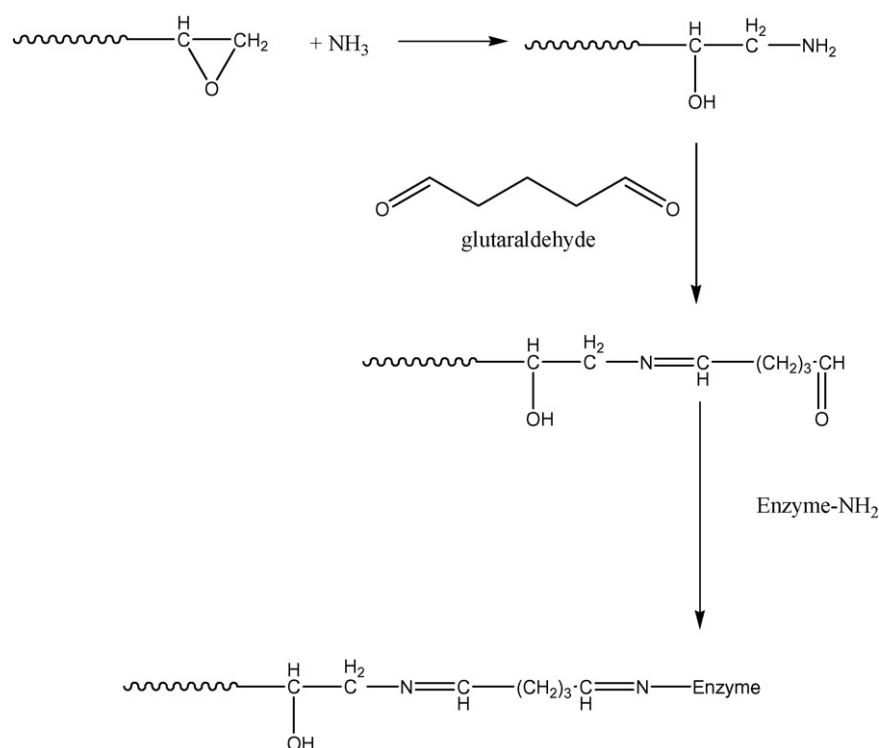
**Scheme 3.** Simple representation for preparations of magnetic beads.

In the second step, magnetic nano-particles encapsulated beads, poly(GMA–MMA), were prepared by co-precipitation. It involves co-precipitation of  $\text{Fe}^{3+}$  and  $\text{Fe}^{2+}$  by adding base, usually NaOH or  $\text{NH}_3 \cdot \text{H}_2\text{O}$ .  $\text{FeCl}_2$  (5.0 g) was dissolved in purified water (100 mL) and transferred into a reactor containing magnetic poly(GMA–MMA) beads (15 g) in  $\text{NH}_3 \cdot \text{H}_2\text{O}$  (50 mL, 25%, w/v). The reactor was equipped with reflux condenser and contents were refluxed under nitrogen atmosphere at three different sequential temperatures (i.e., at 40, 50 and  $90^\circ\text{C}$  for 2 h) while continuous stirring. Finally, the magnetic poly(GMA–MMA) beads were separated from the reaction medium, washed in ethanol solution (50%; 250 mL) for 3 h, and then washed with purified water. The aminated magnetic poly(GMA–MMA) beads (2 g) were transferred to phosphate buffer (pH 7.5; 50 mL), containing 0.5 mL glutaric dialdehyde (50%, w/w).

Reaction was carried out at  $25^\circ\text{C}$  under stirring for 18 h. The activated beads were washed with distilled water, acetic acid solution (0.1 M, 100 mL) and phosphate buffer (50 mM, pH 7.5). The resulting activated beads were sieved and two fractions were (50–75 and 75–150  $\mu\text{m}$  in diameter) used for the covalent immobilization of tyrosinase. Simple representation for the preparation of magnetic beads is shown in Scheme 3.

### 2.3. Enzyme immobilization

The magnetic beads (2 g; 75–150 and/or 50–75  $\mu\text{m}$  in diameter) were washed with 40 mL buffer and equilibrated in 50 mM, pH 7.5 phosphate buffer for 2 h. Glutaraldehyde (5.0%, 0.5 M) was added to the medium, after 18 h reaction period, the unbounded glutaraldehyde



**Scheme 4.** Representation of enzyme immobilization on magnetic beads.

hyde was removed by washing with distilled water and 1.0 M acetic acid. The beads were equilibrated in phosphate buffer and then transferred into the enzyme solution (20 mg tyrosinase in 20 mL phosphate buffer). The immobilization was achieved with a stirring rate of 100 rpm for 12 h at 25 °C. Then the enzyme immobilized magnetic beads were removed from the medium and physically bound enzyme was removed first by washing with saline solution (40 mL, 1.0 M NaCl) and then with phosphate buffer (50 mM, pH 7.0). In these studies a reference support with amino groups carrying magnetic beads were used as a blank support to make sure that final washing eliminates physically bound enzyme molecules.

It was stored at 4 °C in same fresh buffer until use. Schematic representation of enzyme immobilization is shown in Scheme 4. The amount of immobilized tyrosinase on the poly(GMA–MMA) was determined by measuring the initial and final concentrations of protein in the immobilization medium using the Bradford protein determination method.

#### 2.4. Determination of tyrosinase activity

The activity of tyrosinase was determined for both soluble and immobilized enzyme. For the soluble enzyme activity, 2 mL enzyme solution (0.01 M) was added to L-tyrosine solutions with L-ascorbate prepared in the concentration range of 0.5–2.5 mM. The activity of soluble tyrosinase was determined spectrophotometrically. Calibration curve for L-Dopa production was derived using a L-Dopa concentration range between  $10^{-3}$  and  $10^{-6}$  M. For the immobilized tyrosinase activity, three different amounts of magnetic beads were used (5, 10, 20 mg) to determine the optimum amount of magnetic beads in the reaction medium. 10 mg enzyme immobilized beads was found to be suitable for enzymatic assay and 1 h was required to get optimum value of the L-Dopa concentration. After stirring for 1 h, 1.0 mL HCl was added to terminate enzymatic reaction and then 1.0 mL NaOH was added to neutralize the medium. Finally,  $\text{Na}_2\text{MoO}_4$  and  $\text{NaNO}_2$  mixture (1 mL, 15%, w/v) was added and a yellow complex was obtained. Since formation of L-Dopa complex is time dependent, substantial L-Dopa concentrations were determined after 1 h spectroscopically at 460 nm.

#### 2.5. Protein determination

Bradford's method was used for the protein determination of enzyme and the washing solutions [49]. Briefly, a 25 mL phosphoric acid, 12.5 mL ethanol and 25 mg Coomassie Brilliant Blue (G-dye), were mixed to prepare Bradford's reagent. The mixture was diluted to 50 mL by distilled water. A solution of Bradford's reagent was prepared with four volumes of distilled water. Different concentrations of 1.0 mL bovine serum albumin (BSA) were prepared for the protein calibration curve. Diluted Bradford's reagent (2.0 mL) was added to different concentration of BSA solutions. The absorbance values of these solutions were measured at 595 nm.

#### 2.6. Optimum pH and temperature experiments

The effect of pH was determined by changing reaction medium pH between 3.0 and 8.0 at a constant L-tyrosine concentration (0.01 M) for both soluble and immobilized enzyme matrices. The effect of temperature was determined by changing the reaction medium temperature between 20 and 60 °C at constant L-tyrosine concentration. In all experiments the enzyme activity determination was performed as described above, and relative enzyme activity was calculated by assigning the maximum value of activity as 100%.

#### 2.7. Storage and operational stability experiments

The activities of free and immobilized tyrosinase after storage in phosphate buffer (50 mM, pH 7.0) at 4 °C were measured for 3 months in a batch operation mode with the experimental conditions given above.

Operational stability of the immobilized enzyme was studied in a batch system by repetitive uses of the same immobilized enzyme preparation in 50 successive measurements in the same day. In all experiments, relative enzyme activity was calculated by assigning the maximum value of activity as 100%.

### 3. Results and discussion

#### 3.1. Characterization of magnetic beads

Formation of iron oxide in the polymer structure was achieved in two steps: (1) Ferric ions containing poly(GMA–MMA) beads were prepared from monomers via suspension polymerization in the presence of  $\text{Fe}^{3+}$  ions. (2) Classical thermal precipitation reaction was carried out in  $\text{NH}_3$  aqueous solution containing  $\text{Fe}^{2+}$  ions for the formation of iron oxide crystals within the beads. The beads were sieved. Two different fractions with 50–75 and 75–150  $\mu\text{m}$  sizes were produced and used in further reactions. By the BET method, the specific surface areas for both fractions of the magnetic beads were measured as 23.7 and 21.6  $\text{m}^2/\text{g}$ . Using HCl–pyridine method, the amounts of available epoxy groups on the magnetic beads surface were determined as 1.19 and 1.12 mmol/g. GMA was used initially to incorporate epoxy groups on the polymer surface for further modification of the beads. The value obtained for epoxy groups was lower than that of the theoretical value (2.59 mmol/g) since some of the epoxy groups remain inside the magnetic beads and are not accessible for subsequent reactions or analytical determinations. When use of support material in enzyme immobilization is contemplated, the water content is very important. The equilibrium-swelling ratio of the poly(GMA–MMA) beads was determined to be 1.39% on weight basis. This is a moderate swelling ratio and suitable for use as support material for immobilization of different enzymes.

The presence of magnetite nano-particles in the polymeric structure was investigated with an electron spin resonance (ESR) (EL 9, Varian, USA). As presented in Fig. 1 the formation of nano-particles in the beads was confirmed. The intensity of the magnetite peak against magnetic field (Gauss) is also presented in figure. It should be noted that the bare poly(GMA–MMA) beads cannot be magnetized under this condition. The application of an external magnetic field may generate an internal magnetic field in the beads which will add to or subtract from the external field, that is, the local magnetic field generated by the electronic magnetic moment will add vectorially to the external magnetic field ( $H_{\text{ext}}$ ) to give an effective field ( $H_{\text{eff}}$ ) [50]:

$$H_{\text{eff}} = H_{\text{ext}} + H_{\text{local}} \quad (1)$$

As shown in Fig. 1, magnetic poly(GMA–MMA) beads have a relative intensity of  $2.8 \times 10^{-3}$ . This value shows that polymeric structure has a local magnetic field since magnetite nano-particles were formed during thermal precipitation reaction. The  $g$  factor given in Fig. 1 can be considered as a quantity characteristic of the molecules in which the unpaired electrons are located, and it can be calculated from the following equation:

$$g = \frac{h\nu}{\beta H_r} \quad (2)$$

where  $h$  is the Planck constant ( $6.63 \times 10^{-27}$  erg s);  $\beta$  is the universal constant ( $9.27 \times 10^{-21}$  erg/Gs);  $\nu$  is the frequency ( $9.80 \times 10^9$  Hz) and  $H_r$  is resonance of magnetic field (Gs).

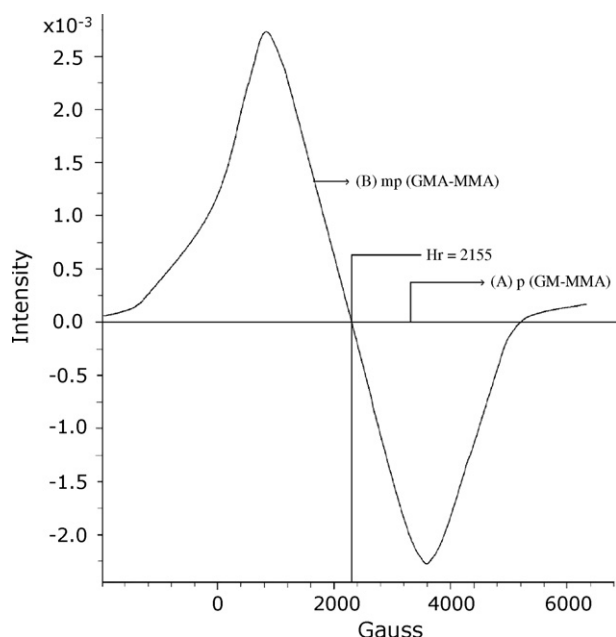


**Fig. 1.** Electron spin resonance (ESR) spectrum of mp (GMA-MMA) beads at room temperature.

The measurement of the  $g$  factor for an unknown signal can be a valuable aid in the identification of a signal. In the literature the  $g$  factor for Fe(III) is the range of 1.4–3.1 for low spin and 2.0–9.7 for high spin complexes [51]. In this study, the  $g$  factor was found to be 3.25 for poly(GMA-MMA) beads. As seen in ESR spectrum and from  $H_r$  value, 2155 Gs magnetic field was found sufficient to excite all of the dipole moments present in 1.0 g of poly(GMA-MMA) beads. In the literature, this value was found to vary from 1000 to 20,000 Gs for various applications, showing that the magnetic beads presented in this study will need less magnetic intensity. The value of this magnetic field is a function of the flow velocity, particle size and magnetic susceptibility of the beads. Hence, the magnetic beads can be easily separated within few seconds by a conventional permanent magnet. When the applied magnetic force is removed the magnetic beads can be easily dispersed by simple shaking. The beads have a spherical form and rough surface due to pores formed during polymerization. The enzyme should be immobilized both on the external surface of the beads and within the pore space near the surface providing a large surface area for the immobilization of tyrosinase. The porous surface properties of the magnetic beads would favor higher immobilization capacity for the enzyme due to increase in the surface area. The enzyme should be immobilized both on the external surface of the magnetic beads and within the pore space near the surface providing a large surface area for the immobilization of tyrosinase. Increasing the porosity of the support provides more area for enzymatic reaction.

The FTIR spectra of magnetic beads have the characteristic vibrations of both GMA and MMA. The methylene vibration exists at  $2957\text{ cm}^{-1}$ , and the peak at  $1735\text{ cm}^{-1}$  represents the ester group for both MMA and GMA. The epoxide group gives a band  $971\text{ cm}^{-1}$ .

The characteristic band at  $600\text{ cm}^{-1}$  indicates that  $\text{Fe}_3\text{O}_4$  molecules are successfully formed within the structure of poly(GMA-MMA) beads [41].

### 3.2. Enzyme loading on the magnetic beads

The covalent immobilization of commercially important enzyme, tyrosinase, was studied via glutaraldehyde coupling using two different size fractions of magnetic beads. According to the data obtained using Bradford method, the amounts of immobilized protein were found as 2.7 and 2.8 mg protein/g magnetic beads for 50–75 and 75–150  $\mu\text{m}$  fractions, respectively (Table 1).

### 3.3. Kinetic parameters of soluble and immobilized enzyme

Mechanisms that influence the interactions between biological substrates and enzymes are essential to engineer biomolecular processes. During the last few decades, considerable research efforts have been directed to understand the mechanisms of enzyme functions [51]. Enzymatic assay mentioned in Section 2.4 was applied to both soluble and immobilized enzyme matrices with preset concentrations of L-tyrosine.  $V_{\text{max}}$  and  $K_m$  values were determined from Lineweaver-Burk plot at  $25^\circ\text{C}$  and pH 7.0. The parameters were given in Table 1. As seen in this table, the  $V_{\text{max}}$  values for 50–75 and 75–150  $\mu\text{m}$  magnetic beads were found as  $2.9 \times 10^{-3}$  and  $5.6 \times 10^{-3}$  ( $\mu\text{mol}/(\text{min mg (bead)})$ ). As regards to the amount of immobilized protein from Bradford method  $V_{\text{max}}$  values can be calculated as 1.05 and 2.00 in terms of  $\mu\text{mol}/(\text{min mg (protein)})$  for 50–75 and 75–150  $\mu\text{m}$  fractions. Increase in the bead size (i.e., from 50–75 to 75–150  $\mu\text{m}$  fraction) resulted in an enhanced enzyme activity. The enzyme immobilized magnetic beads of 75–150  $\mu\text{m}$  fraction shows better response than other matrix. Also,  $K_m$  values which show the affinity towards substrate decreased for both matrices compared to the one for soluble enzyme. For 50–75  $\mu\text{m}$  magnetic beads there exists a substrate diffusion limitation since as the bead size decreases the pore size on the beads also decreases. Thus, enzyme could not match with required amounts of its substrate due to substrate diffusional limitations causing a decrease in  $V_{\text{max}}$ . Moreover, the conformations of the enzyme have changed due to immobilization since after immobilization; enzyme seems to have a true higher affinity for the substrate with 50–75  $\mu\text{m}$  magnetic beads, though not a higher activity. For 75–150  $\mu\text{m}$  fraction magnetic beads it seems like the affinity is for the substrate is low, but whenever the enzyme-substrate come together they produce the product. This is resulted in high  $V_{\text{max}}$  for 75–150  $\mu\text{m}$  fraction. Thus, 75–150  $\mu\text{m}$  fraction magnetic beads reveal more reasonable  $V_{\text{max}}$  and  $K_m$  values than that of the soluble enzyme and the enzyme immobilized on the 50–75  $\mu\text{m}$  bead fractions. Similar findings were reported in the literature [52]. 75–150  $\mu\text{m}$  fraction magnetic beads immobilized enzyme system provided an efficiency factor ( $\eta$ ) of 1.39 for the immobilized tyrosinase and  $\eta$  was found as 0.73 for 50–75  $\mu\text{m}$  beads fractions. The ratio of  $V_{\text{max}}$  to  $K_m$  defines the catalytic efficiency ( $k_b$ ) of an enzyme-substrate pair. Catalytic efficiency of the soluble tyrosinase was calculated as 0.37. This value is 0.75 for 50–75 and 0.91 for 75–150  $\mu\text{m}$  fractions. The catalytic efficiency of the 75–150 and 50–75  $\mu\text{m}$

**Table 1**

Properties of the soluble and immobilized tyrosinase on the magnetic beads.

Form of enzyme	$K_m$ (mM)	$V_{\text{max}}$ ( $\mu\text{mol}/(\text{min mg (protein)})$ )	Enzyme loading (mg enzyme/g beads)	Efficiency factor ( $v_{\text{immobilized}}/v_{\text{free}}$ )	Catalytic efficiency ( $V_{\text{max}}/K_m$ )
Free enzyme	3.9	1.43	–	–	0.37
Immobilized enzyme on 50–75 $\mu\text{m}$ fraction	1.4	1.05	2.7	0.73	0.75
Immobilized enzyme on 75–150 $\mu\text{m}$ fraction	2.2	2.00	2.8	1.39	0.91



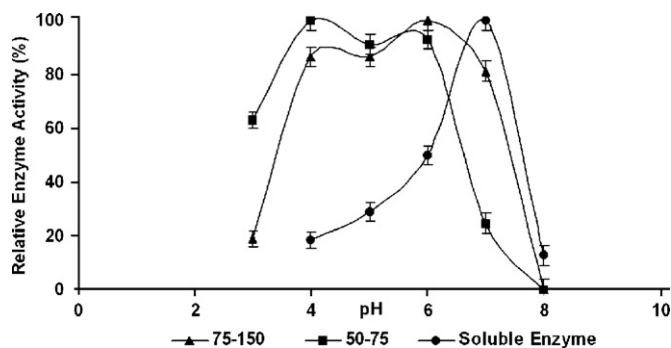


Fig. 2. Effect of pH on soluble enzyme, 50–75 and 75–150  $\mu\text{m}$  fraction magnetic beads matrices.

fractions increased 2.46- and 2.02-fold, respectively upon immobilization.

### 3.4. Effect of pH

As shown in Fig. 2, magnetic bead matrices have enzymatic activity in a wide pH range. As the pH increased relative activity also increased at low pH values. At higher pH, relative enzyme activities were decreased for both immobilized matrices. While soluble enzyme presented maximum activity at pH 7 with a sharp drop at more acidic and basic pH values, immobilized enzymes presented a better pH activity profile, with a values over 80% between pH 4 and 8. As an advantage, immobilized enzyme matrices reveal enzymatic activity in a wider pH range than that of soluble enzyme matrix. This makes the new biocatalysts more suitable for use.

### 3.5. Effect of temperature

The influences of temperature on the activity of magnetic beads were given in Fig. 3. Relative enzyme activity was calculated by assigning the maximum activity value as 100%. The temperature profile of the immobilized tyrosinase was broader at high temperature compared to the soluble enzyme. At low temperatures, the catalytic activity of both types of the magnetic bead matrices increased with the rise of the temperature at first and after a maximum (at 40 °C for each matrices), decreased at a higher temperature. For soluble enzyme the optimal temperature was found to be 30 °C and there exist sharp increase and decrease before and after 30 °C. As it was evident from the data, the immobilized enzyme reveals a better heat-resistance than soluble enzyme. The immobilization procedure could protect the enzyme active conformation from distortion or damage by heat exchange. One of the main reasons for enzyme immobilization is the anticipated increase in its stability to various deactivating factors due to restricted confor-

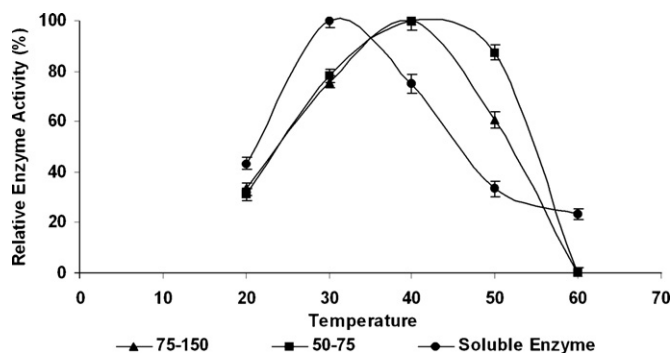


Fig. 3. Effect of temperature on soluble enzyme, 50–75 and 75–150  $\mu\text{m}$  fraction magnetic bead matrices.

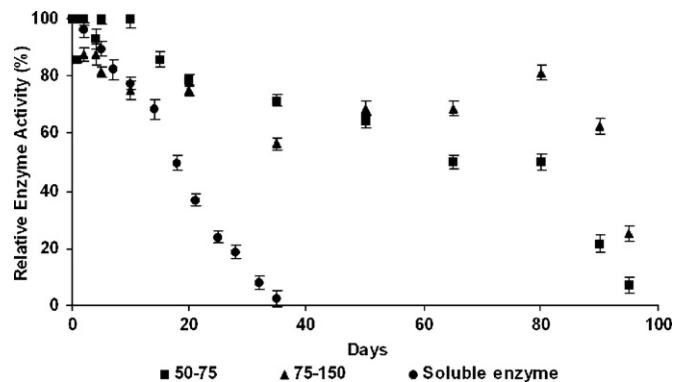


Fig. 4. Storage stabilities of soluble enzyme, 50–75 and 75–150  $\mu\text{m}$  fraction magnetic bead matrices.

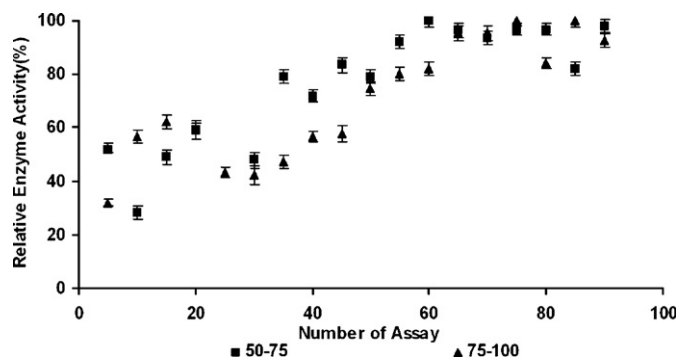


Fig. 5. Operational stabilities of soluble enzyme, 50–75 and 75–150  $\mu\text{m}$  fraction magnetic bead matrices.

mational mobility of the molecules after immobilization [53,54]. Therefore, the immobilized enzyme could work in harsh environmental conditions with lower activity loss compared to the soluble counterpart. Since human body temperature is around 37 °C, 75–150  $\mu\text{m}$  fraction magnetic beads which have maximum activity at 40 °C present more reliable results than 50–75  $\mu\text{m}$  fraction magnetic beads.

### 3.6. Storage and operational stability

The main problem in using enzymes on productive scale is their stability. Stability of immobilized enzyme is an important parameter since enzymes can easily be denatured. Concerning the stability good storage and operational stability parameters are essential. At the 90th day, the immobilized enzyme matrix for 75–150  $\mu\text{m}$  fraction magnetic beads shows 5% activity whereas this is 20% for 50–75  $\mu\text{m}$  fraction magnetic beads as shown in Fig. 4. There exists a decrease in the activity by 50% after 35 days and then, due to the conformation and stability changes activity decreases sharply. It is clear that the activity of the soluble enzyme decreases faster in nearly 4 weeks, than the immobilized tyrosinase on magnetic beads under the same storage conditions. In operational stability experiments, there exists a remarkable increase in the concentration of the L-Dopa (Fig. 5). The matrices enhance the enzymatic activity causing an increase in the production of L-Dopa as shown in Fig. 5. Thus, magnetic beads with immobilized enzyme continuously produce L-Dopa.

## 4. Conclusion

L-Dopa is the immediate precursor of the natural neurotransmitter, dopamine, and is widely used as medication for Parkinson's

disease to improve the symptoms due to decreased dopamine levels. To synthesize L-Dopa, poly(GMA–MMA) beads were prepared from GMA and MMA via suspension polymerization and tyrosinase was covalently immobilized on the magnetic beads. The poly(GMA–MMA) beads have numerous advantages such as preparing the reactive beads without any activation steps. They can be used for enzyme immobilization under mild experimental conditions. They have high enzyme binding capacity due to the highly porous surface structure. They can form the desired amount of epoxy on the beads' surface by changing the monomer ratio in the initial polymerization mixture. Kinetic parameters ( $V_{\max}$ ,  $K_m$ ) were determined for the 50–75 and 75–150  $\mu\text{m}$  fractions of the magnetic beads.  $V_{\max}$  is 1.05 for 50–75 and 2.00  $\mu\text{mol}/(\text{min mg (protein)})$  for 75–150  $\mu\text{m}$  fractions.  $K_m$  values are 1 and 4 mM, respectively. Catalytic efficiency is 0.75 for 50–75  $\mu\text{m}$  and 0.91 for 75–150  $\mu\text{m}$  fractions whereas it is 0.37 for the soluble enzyme. Thus, the catalytic efficiency increased at least twice upon immobilization. Temperature, pH, operational and storage stability, experiments were performed to characterize immobilized enzyme matrices. Hence, an alternative route for synthesizing L-Dopa was achieved.

### Acknowledgement

This work is partially supported by TUBA grant.

### References

- [1] Y. Misu, Y. Goshima, T. Miyamae, Trends Pharmacol. Sci. 23 (2002) 262–268.
- [2] W.S. Knowles, Adv. Synth. Catal. 345 (2003) 3–13.
- [3] P. Pialis, B.A. Saville, Enzyme Microb. Technol. 22 (1998) 261–268.
- [4] F. Stocchi, N.P. Quinn, L. Barbato, P.N. Patsalos, M.T. O'Connell, S. Ruggieri, C.D. Marsden, Clin. Neuropharmacol. 17 (1994) 38–44.
- [5] P. Damier, E.C. Hirsch, Y. Agid, A.M. Graybiel, Brain 122 (1999) 1437–1448.
- [6] B.B. Azad, R. Chirakal, G.J. Schrobilgen, J. Label. Compd. Radiopharm. 50 (2007) 1236–1242.
- [7] H.W. Duckworth, J.E. Coleman, J. Biol. Chem. 245 (1970) 1613–1625.
- [8] B.S. Aytar, U. Bakir, Process Biochem. 43 (2008) 125–131.
- [9] M. Perez-Gilabert, F. Garcia-Carmona, Biochem. Biophys. Res. Commun. 285 (2001) 257–263.
- [10] C.J. Cooksey, P.J. Garratt, E.J. Land, S. Pavel, C.A. Ramsden, P.A. Riley, N.P. Smit, J. Biol. Chem. 272 (1997) 26226–26235.
- [11] H.S. Raper, J. Biochem. 21 (1927) 89–96.
- [12] H. Fedorow, F. Tribl, G. Halliday, M. Gerlach, P. Riederer, K.L. Double, Prog. Neurobiol. 75 (2005) 109–124.
- [13] J.R. Ros, J.N. Rodriguez-Lopez, G.F. Conovas, Biochem. J. 295 (1993) 309–312.
- [14] A. Arslan, S. Kiralp, L. Toppare, A. Bozkurt, Langmuir 22 (2006) 2912–2915.
- [15] S. Tuncagil, S. Kiralp, S. Varis, L. Toppare, React. Func. Polym. 68 (2008) 710–717.
- [16] H.B. Yildiz, S. Kiralp, L. Toppare, Y. Yagci, Int. J. Biol. Macromol. 37 (2005) 174–178.
- [17] S. Alacam, S. Timur, A. Telefoncu, J. Mol. Catal. B 49 (2007) 55–60.
- [18] R. Baron, M. Zayats, I. Willner, Anal. Chem. 77 (2005) 1566–1571.
- [19] P. Pialis, J. Hamann, B. Saville, Biotechnol. Bioeng. 51 (1996) 141–147.
- [20] S. Ates, E. Cortenlioglu, E. Bayraktar, U. Mehmetoglu, Enzyme Microb. Technol. 40 (2007) 683–687.
- [21] G. Seetharam, B.A. Saville, Enzyme Microb. Technol. 31 (2002) 747–753.
- [22] E. Vilanova, A. Monjan, J.L. Iborra, Biotechnol. Bioeng. 26 (1984) 1306–1312.
- [23] N. Munjal, S.K. Sawhney, Enzyme Microb. Technol. 30 (2002) 613–619.
- [24] P.Y. Ho, M.S. Chiou, A.C. Chao, Appl. Biochem. Biotechnol. 111 (2003) 139–152.
- [25] C. Acharya, V. Kumar, R. Sen, S.C. Kundu, Biotechnol. J. 3 (2008) 226–233.
- [26] M. Filho, B.C. Pessela, C. Mateo, A.V. Carrascosa, R. Fernandez-Lafuente, J.M. Guisan, Enzyme Microb. Technol. 42 (2008) 265–271.
- [27] C. Mateo, O. Abian, R. Fernandez-Lafuente, J.M. Guisan, Enzyme Microb. Technol. 46 (2007) 509–515.
- [28] L. Betancor, F. Lopez-Gallego, A. Hidalgo, N. Alonso-Morales, G. Dellamora-Ortiz, C. Mateo, R. Fernández-Lafuente, J.M. Guisan, Enzyme Microb. Technol. 39 (2006) 877–882.
- [29] C. Mateo, J.M. Palomo, G. Fernandez-Lorente, J.M. Guisan, R. Fernandez-Lafuente, Enzyme Microb. Technol. 40 (2007) 1451–1463.
- [30] F. Lopez-Gallego, L. Betancor, C. Mateo, A. Hidalgo, N. Alonso-Morales, G. Dellamora-Ortiz, J.M. Guisan, R. Fernandez-Lafuente, J. Biotechnol. 119 (2005) 70–75.
- [31] R. Fernandez-Lafuente, V. Rodriguez, J.M. Guisan, Enzyme Microb. Technol. 23 (1998) 28–33.
- [32] J.M. Guisan, Enzyme Microb. Technol. 10 (1988) 375–382.
- [33] J.M. Guisan, A. Bastida, C. Cuesta, R. Fernandez-Lafuente, C.M. Rosell, Biotechnol. Bioeng. 39 (1991) 75–84.
- [34] V.V. Mozhaev, A.M. Klibanov, V.S. Goldmacher, I.V. Berezin, Biotechnol. Bioeng. 25 (1990) 1937–1945.
- [35] G. Bayramoglu, S. Kiralp, M. Yilmaz, L. Toppare, M.Y. Arica, Biochem. Eng. J. 38 (2008) 180–188.
- [36] S. Libertino, F. Giannazzo, V. Aiello, A. Scandurra, F. Sinatra, M. Renis, M. Fichera, Langmuir 24 (2008) 1965–1972.
- [37] R.L. Palomo, G. Segura, R. Fernandez-Lorente, J.M. Fernandez-Lafuente, J.M. Guisán, Enzyme Microb. Technol. 40 (2007) 704–707.
- [38] G. Bayramoglu, E. Logoglu, M.Y. Arica, Colloid Surf. A 297 (2007) 55–62.
- [39] H.A. Oktem, G. Bayramoglu, V.C. Ozalp, M.Y. Arica, Biotechnol. Prog. 23 (2007) 146–154.
- [40] H. Boa, Z. Chen, L. Kang, P. Wu, J. Liu, Mater. Lett. 60 (2006) 2167–2170.
- [41] M.Y. Arica, Y. Tunalı, G. Bayramoglu, Catal. Commun. 8 (2007) 1094–1101.
- [42] S. Lu, J. Forcada, J. Polym. Sci. A: Polym. Chem. 44 (2006) 4187–4203.
- [43] J. Hong, P.J. Gong, J.H. Yu, D.M. Xu, H.W. Sun, S. Yao, J. Mol. Catal. B 42 (2006) 99–105.
- [44] S. Kiralp, A. Topcu, G. Bayramoglu, M.Y. Arica, L. Toppare, Sensors Actuat. B: Chem. 128 (2008) 521–528.
- [45] L. Betancor, M. Fuentes, G. Dellamora-Ortiz, F. Lopez-Gallego, A. Hidalgo, N. Alonso-Morales, C. Mateo, J.M. Guisan, R. Fernandez-Lafuente, J. Mol. Catal. B: Enzym. 32 (2005) 97–101.
- [46] S.-F. Li, J.-P. Chen, W.-T. Wu, J. Mol. Catal. B: Enzym. 47 (2007) 117.
- [47] J. Hong, P. Gong, D. Xu, L. Dong, S. Yao, J. Biotechnol. 128 (2007) 597.
- [48] X. Liu, Y. Guan, R. Shen, H. Liu, J. Chromatogr. B 822 (2005) 91.
- [49] M. Bradford, Anal. Biochem. 72 (1976) 248–254.
- [50] Z. Guo, Y. Sun, Biotechnol. Prog. 20 (2004) 500–506.
- [51] H.M. Swartz, J.R. Bolton, D.C. Borg, Biological Applications of Electron Spin Resonance, second ed., Wiley Interscience, New York, 1972.
- [52] X. Turon, O.J. Rojas, R.S. Deinhammer, Langmuir 24 (2008) 3880–3887.
- [53] L.E. Wierzbicki, V.H. Edwards, F.V. Kosikowski, J. Food Sci. 38 (1974) 1070–1073.
- [54] M.Y. Arica, G. Bayramoglu, J. Mol. Catal. B: Enzym. 38 (2006) 131–138.